Hindawi Publishing Corporation
Mathematical Problems in Engineering
Volume 2013, Article ID 517608, 11 pages
http://dx.doi.org/10.1155/2013/517608

Research Article

Wide-Area H_∞ Control for Damping Interarea Oscillations with Event-Triggered Scheme

Yunning Zhang,[1,2] Dong Yue,[1] and Songlin Hu[3]

[1] *Department of Control Science and Engineering, Huazhong University of Science and Technology, Wuhan, Hubei 430074, China*
[2] *College of Electrical Engineering and New Energy, China Three Gorges University, Yichang, Hubei 443002, China*
[3] *College of Mathematics and Computer Science, Hubei University of Arts and Science, Xiangyang, Hubei 441053, China*

Correspondence should be addressed to Dong Yue; medongy@vip.163.com

Received 12 January 2013; Accepted 4 March 2013

Academic Editor: Engang Tian

An event-triggered scheme is adopted and applied to the design of a centralized wide-area H_∞ damping controller (WAHDC) of interconnected power systems with external disturbance. Firstly, based on the linearized multimachine system model, the centralized WAHDC with event-triggered scheme design problem is described as time-delay feedback control problem. Then by using Lyapunov functional method and Jensen inequality technique, criteria for stability with an H_∞ norm bound and for design of the feedback controller are derived. The linear matrix inequality (LMI) is employed to solve the feedback gain. Finally, case studies are carried out based on two-area four-machine power system. Simulations indicate that the proposed WAHDC with event-triggered scheme can damp the interarea oscillation effectively when the external disturbance is bounded and significantly reduce the number of measured states released to WAHDC. Relationships between event trigger parameter σ and dynamic performance, σ and network utilization, σ and time delay, and σ and disturbance rejection level are investigated and results obtained can be used to choose an appropriate event trigger parameter.

1. Introduction

Interarea oscillations are the manifestation of consequences of small disturbances in weakly interconnected power systems [1]. The phenomenon is not new. However, it has evolved from being a local problem to becoming a global one. As more regional power systems are integrated for higher reliability and economy of scale, low frequency interarea oscillations have become one of the major challenges to the power system operators. This type of oscillations limits the amount of power transfer on the tie lines between the regions containing coherent generator groups [2].

The traditional approach to damping out interarea oscillations is to install power system stabilizers (PSSs) that provide supplementary control action through the generator excitation systems [2]. The input of PSS is often local signal. Such PSS is effective in damping local modes. While for wide-area complex power systems, the effectiveness in damping interarea modes is limited. It has been proved that under certain operating conditions an interarea mode may be controllable from one area and be observable from another [3]. In such cases, local PSSs are not effective for the damping of that mode. Proposed solutions to interarea oscillation damping control range from new PSS design [4], including multiband PSS concept [5] H_∞-approach-based supervisory-level PSS [6], to control systems that deploy wide-area measurement systems (WAMSs) [7–10]. With the technology of phasor measurement units (PMUs), WAMS allows to synchronized signals measured at remote locations to be available in real time in the control center.

The overall objective of WAMS is to provide dynamic power system measurements. Except for damping control mentioned previously, WAMS can also provide complete monitoring, protection, and control of the power system. Reference [11] presents a sectionalizing method based on WAMS for the build-up strategy in power system restoration. Reference [12] uses globally measured output signals to estimate reduced order state-space models of large power systems with many controllable devices for subspace system

identification. Based on the WAMS output of a power system, [13] presents a new methodology to construct power system area load models alongside network reduction. In [14], a fault location method based on principal component analysis is proposed, in which synchronized information data are utilized provided by the WAMS/PMU measurement system. In order to improve the precision, the literature [15] constructs a state estimation objective function combined with the constraints of zero-injection nodes and WAMS.

One can imagine that, with the development of the technology and with a detailed study, WAMS will be used more and more widely in deregulated power systems. It brings a lot of opportunities for improving system stability, but also huge challenges such as the communication pressure to network by remote magnanimity data transmission. However, periodic sample and control strategy will lead to the sending of many redundant signals through network as mentioned in [16–19]. About how to reduce communication requirements on network control systems, other sample and control strategies have appeared in the literature [20–25]. References [26, 27] introduce trigger scheme in excitation control of single machine and state estimation of multiarea power system. As pointed out in [28], although these schemes have different triggering conditions, they are based on a similar concept that the signal will be released to network only "when needed." Different from those "sampled when needed" strategies, Yue et al. propose a novel event-triggered scheme in [16–19]. It uses a periodic sample scheme, but an evaluation of whether every sample fulfils a certain condition should be taken before the sampled signals are sent to the network. In that case, the number of signals to be transmitted to the controller can be reduced. And in turn, the number of control output calculations can decrease. Therefore the network bandwidth can be used fully and the computation load at the controller can be relieved.

In order to enhance the dynamic performance of power systems and make full use of constrained bandwidth of WAMS at the same time, this paper investigates a wide-area H_∞ damping controller (WAHDC) design with event-triggered scheme and some related issues about the possible implement method in electrical power engineering. As centralized wide-area damping control provides more efficient solutions due to the availability of large amount of system-wide dynamic data and better observation of interarea modes [2], to improve the damping performance, centralized wide-area full state feedback is introduced based on WAMS. For the feature that machines are distributed widely in multimachine power system, different from [16–19] in which an event generator is located at the sampler side, an event detector sited between PMU and WAHDC at the control center is used to determine whether the newly measured state should be released to WAHDC, but every measured signal by PMU will be sent to the event detector through network. Based on a similar model proposed in [16–19], criteria for the stability with an H_∞ norm bound and controller design are set and expressed in the form of linear matrix inequality (LMI). For the purpose of dealing with the uncertainty introduced by external disturbance, H_∞ control method is adopted [29]. Simulation results show the effectiveness of WAHDC with event-triggered scheme and also provide a possible method to choose appropriate event trigger parameter to get trade-off to balance the damping performance, utilization of communication and computation resources, delay margin, and disturbance rejection level.

The remainder of the paper is organized as follows. In Section 2, the problem under consideration is formulated after the modeling of multimachine power system. The centralized H_∞ excitation control performance analysis and synthesis results are studied in Section 3. Case studies are presented in Section 4 using a benchmark two-area four-machine power system controlled by WAHDC with event-triggered scheme. Simulation example is provided to demonstrate the effectiveness of the proposed control scheme. What is more, the relationships between event trigger parameter σ and damping performance, σ and delay margin, and σ and disturbance rejection level are investigated, respectively, in this section. Finally, the conclusions are presented in Section 5.

2. System Modeling and Problem Formulation

2.1. Small Signal Model of Multimachine Power Systems. Generally speaking, low frequency oscillation is a typical problem of small-signal stability. Small-signal (or small-disturbance) stability is the ability of the power system to maintain synchronism under small disturbances. The disturbances are considered to be small and usually will not lead to structure and operating point change of the power systems. For the purpose of analysis, the equations that describe the resulting response of the system may be linearized at certain operating point [30].

Consider a multimachine power system composed of n generators. The generator is represented by the third-order model. Assuming the input mechanical torque is constant, that is, neglecting the influence of the governor system, assuming the excitation system is separative stationary controllable silicone excitation system and ignoring the time constants of power unit and excitation regulator, and taking the excitation voltage deviation ΔE_f as excitation control input, the equation of each generator is expressed as follows [31]. The physical meaning of the corresponding parameters is listed in list of symbols:

$$\begin{aligned}
\dot{\delta}_i(t) &= \omega_i(t) - \omega_0 \\
\dot{\omega}_i(t) &= \frac{\omega_0}{M_i} P_{mi} - \frac{D_i}{M_i}\left(\omega_i(t) - \omega_0\right) - \frac{\omega_0}{M_i} P_{ei} \\
\dot{E}'_{qi}(t) &= -\frac{1}{T'_{d0i}}\left[E'_{qi}(t) + I_{di}\left(x_{di} - x'_{di}\right)\right] + \frac{1}{T'_{d0i}} E_{fi},
\end{aligned} \tag{1}$$

where

$$\begin{aligned}
P_{ei} &= \left[E'_{qi}(t) + I_{di}\left(x_{qi} - x'_{di}\right)\right] I_{qi}, \\
I_{di} &= \sum_{j=1}^{n} E'_{qj}(t)\left[G_{ij}\cos\delta_{ij} - B_{ij}\sin\delta_{ij}\right], \\
I_{qi} &= \sum_{j=1}^{n} E'_{qj}(t)\left[G_{ij}\sin\delta_{ij} + B_{ij}\cos\delta_{ij}\right].
\end{aligned} \tag{2}$$

$i, j = 1, 2, \ldots, n$. $\delta_{ij} = \delta_i - \delta_j$ denotes relative power angle between the ith and the jth generators. Other parameters are introduced in list of symbols. Taking $x = \left[\Delta\delta \;\; \Delta\omega \;\; \Delta E'_q\right]^T$ as the state vector, applying Taylor series approximation at the given operating point, and then rearranging appropriately, linearized model of n-machine power system can be written as [32]

$$\dot{x} = A_1 x + B_1 u, \tag{3}$$

where

$$\begin{aligned}
\Delta\delta &= \left[\Delta\delta_1 \;\; \Delta\delta_2 \;\; \cdots \;\; \Delta\delta_n\right]^T,\\
\Delta\omega &= \left[\Delta\omega_1 \;\; \Delta\omega_2 \;\; \cdots \;\; \Delta\omega_n\right]^T,\\
\Delta E'_q &= \left[\Delta E'_{q1} \;\; \Delta E'_{q2} \;\; \cdots \;\; \Delta E'_{qn}\right]^T,\\
u &= \Delta E_f,\\
\Delta E_f &= \left[\Delta E_{f1} \;\; \Delta E_{f2} \;\; \cdots \;\; \Delta E_{fn}\right]^T,
\end{aligned} \tag{4}$$

$$A_1 = \begin{bmatrix} 0 & I & 0 \\ -\dfrac{K_1}{M} & -\dfrac{D}{M} & -\dfrac{K_2}{M} \\ -\dfrac{1}{T'_{d0}}K_3 & 0 & -\dfrac{1}{T'_{d0}}K_4 \end{bmatrix}, \tag{5}$$

$$B_1 = \begin{bmatrix} 0 & 0 & 0 & \dfrac{1}{T'_{d0}} \end{bmatrix}^T, \tag{6}$$

where

$$\begin{aligned}
M &= \operatorname{diag}\{M_1, M_2, \ldots, M_n\}\\
D &= \operatorname{diag}\{D_1, D_2, \ldots, D_n\}\\
T'_{d0} &= \operatorname{diag}\left\{T'_{d01}, T'_{d02}, \ldots, T'_{d0n}\right\}\\
K_1 &= \frac{\partial P_e}{\partial \delta},\\
K_2 &= \frac{\partial P_e}{\partial E'_q},\\
K_3 &= \frac{\partial\left[E'_q + \left(x_q - X'_d\right) I_d\right]}{\partial E'_q},\\
K_4 &= \partial\frac{\left[E'_q + \left(x_q - X'_d\right) I_d\right]}{\partial \delta}.
\end{aligned} \tag{7}$$

For convenience of excitation controller design, one can choose the nth machine as the reference one, and the state vector is reselected as $x = \left[x_1 \;\; x_2 \;\; \cdots \;\; x_n\right]^T$, where $x_i = \left[\Delta\delta_{in} \;\; \Delta\omega_i \;\; \Delta E'_{qi}\right]^T$, $i = 1, 2, \ldots, n-1$. $x_n = \left[\Delta\omega_n \;\; \Delta E'_{qn}\right]^T$. By some mathematical similarity transformation and considering the disturbance entering the excitation winding, one can get the state-space description of n-machine system as

$$\dot{x}(t) = Ax(t) + Bu(t) + B_2\varepsilon(t), \tag{8}$$

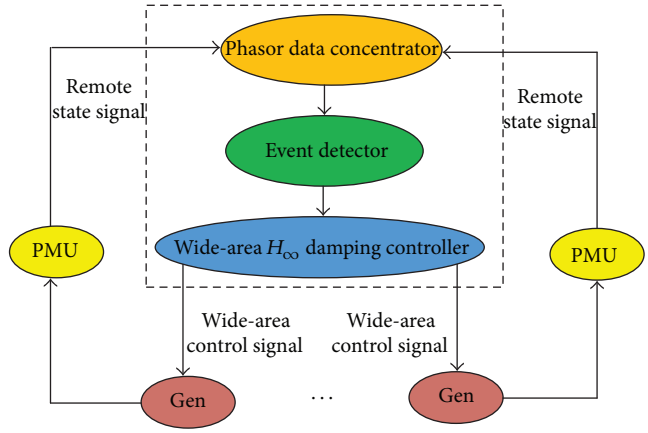

Figure 1: General structure of wide-area damping control system with event-triggered scheme.

where $\varepsilon(t) = \left[\varepsilon_1(t) \;\; \varepsilon_2(t) \;\; \cdots \;\; \varepsilon_n(t)\right]^T$ denotes the disturbance signal and $\varepsilon(t) \in L_2[0, +\infty]$. A, B, and B_2 are constant matrices with appropriate dimensions, and A, B can be obtained from (3) by some simple matrix similarity transformation. Note that the order of (8) is one order less than (3); that is, the order of (8) is $3n - 1$.

2.2. System Description of Wide-Area Damping Control. For the problem of wide-area H_∞ damping control, one can choose a regulated output vector as $z(t)$; thus the multimachine power system considered here can be described as

$$\begin{aligned}
\dot{x}(t) &= Ax(t) + Bu(t) + B_2\varepsilon(t),\\
z(t) &= Cx(t) + Du(t),
\end{aligned} \tag{9}$$

where C and D are weighting matrices and $u(t)$ is constructed by the linear combination of state signals sampled by remote PMU.

As is known, periodic controlling mechanism may often lead to the sending of many redundant signals through the communication network of WAMS, which will in turn increase the load of network transmission and waste the network bandwidth. Therefore, it is significant to introduce a mechanism to decide which sampled state signals should be taken to calculate the control output. A pretreatment mechanism called event detector (ED) is constructed in the wide-area damping control loop located after the phasor data concentrator (PDC) at the control center. If a signal is sent to the WAHDC, we define that an event happens. The framework of WAMS-based wide-area damping control with event-triggered scheme is shown in Figure 1. Focusing on the closed-loop framework shown in Figure 1, the following functionality is expected.

(i) The controlled machines are sampled simultaneously by different PMUs with the sampling period h, which can be obtained by global positioning system (GPS) inducing time function. The time of the kth sampling is written as kh, $k = 0, 1, 2, \ldots, \infty$. For simplifying the analysis, assume all of the measured signals are time

stamped and arrive at the event detector at the same time. Meanwhile, we also assume that the delays from the controller to the actuators distributed widely are the same.

(ii) If the kth sampled state signal is taken to calculate the control output, the instant will be marked as $t_m h$, $m = 0, 1, 2, \ldots, \infty$. Then the released time at the ED is $t_m h + \tau_{sc}(m)$. The meaning of the notation $\tau_{sc}(m)$ will be depicted later. The ED uses the previously transmitted sampled data $x(t_m h)$ to decide whether the current sampled data $x((k+j)h)$ $(j \in 1, 2, \ldots, \infty)$ needs to be released based on the following quadratic condition, that is, the event-triggered release scheme

$$\begin{aligned}&\left[x\left(\left(k+j\right)h\right) - x\left(t_m h\right)\right]^T \Omega \left[x\left(\left(k+j\right)h\right) - x\left(t_m h\right)\right] \\ &\leq \sigma x^T\left(\left(k+j\right)h\right) \Omega x\left(\left(k+j\right)h\right),\end{aligned} \tag{10}$$

where Ω is a positive matrix and $\sigma \geq 0$. The current sampled signal $x((k+j)h)$ will not be released to calculate the control action if condition (10) is satisfied. In other words, only the sampled signals that violate condition (10) will be released by ED to calculate the control output. Assume the signal sampled at the initial time is released, which means $t_0 h = 0$. In particular, when $\sigma = 0$, all the sampled signals are transmitted to the control center and used to calculate control action. Then the event-triggered scheme reduces to the periodic sampling and controlling scheme.

(iii) When the signal has been sampled by PMU, it is forwarded to the control center, introducing a sensor-to-controller delay $\tau_{sc}(m)$. It is noteworthy that $\tau_{sc}(m)$ can be obtained with the time stamp and the synchronization measurement feature of PMU. The controller forwards the actuation signals to the actuators, introducing another communication delay, controller-to-actuator delay $\tau_{ca}(m)$, which includes the time delay introduced by control output computation. The total transmission time delay can be lumped together as $\tau_m = \tau_{sc}(m) + \tau_{ca}(m)$, $\tau_m \in (0, \overline{\tau}]$, where $\overline{\tau}$ is a positive real number. Finally, the actuators perform the actuation at the time given by $t_m h + \tau_m$.

Based on the previous analysis, considering the effect of the transmission delay, the system model with event-triggered scheme can be described as

$$\begin{aligned}\dot{x}\left(t\right) &= Ax\left(t\right) + Bu\left(t_m h\right) + B_2 \varepsilon\left(t\right), \\ z\left(t\right) &= Cx\left(t\right) + Du\left(t_m h\right), \\ t &\in \left[t_m h + \tau_m, t_{m+1} h + \tau_{m+1}\right).\end{aligned} \tag{11}$$

For the ease of analysis, for $t \in [t_m h + \tau_m, t_{m+1} h + \tau_{m+1})$, the system (11) can be converted to a time-delay system using similar methods in [17, 19]

$$\dot{x}\left(t\right) = Ax\left(t\right) + BKx\left(t - \tau\left(t\right)\right) + BKe_m\left(t\right) + B_2 \varepsilon\left(t\right) \tag{12}$$

$$z\left(t\right) = Cx\left(t\right) + DKx\left(t - \tau\left(t\right)\right) + DKe_m\left(t\right) \tag{13}$$

$$x\left(t\right) = \phi\left(t\right), \quad t \in \left[-\tau_M, 0\right], \tag{14}$$

where $\phi(t)$ is the initial time of $x(t)$. $\tau_M = h + \overline{\tau}$, and the definition of $e_m(t)$ is the same as $e_k(t)$ in [19]. Correspondingly, the event-triggered condition is converted as

$$e_m^T\left(t\right) \Omega e_m\left(t\right) \leq \sigma x^T\left(t - \tau\left(t\right)\right) \Omega x\left(t - \tau\left(t\right)\right). \tag{15}$$

2.3. Problem Formulation. The purpose of the paper is to develop techniques to deal with H_∞ event-triggered control problem for n-machine power system (12)–(14) based on WAMS. For a given scalar $\gamma > 0$, the performance of system (12)–(14) is defined to be

$$J\left(\varepsilon\right) = \int_0^\infty \left[z^T\left(t\right) z\left(t\right) - \gamma^2 \varepsilon^T\left(t\right) \varepsilon\left(t\right)\right] dt. \tag{16}$$

Then the H_∞ event-triggered control problem addressed in this paper can be stated so as to design a state feedback controller such that system (12)–(14) under the event detector with event triggering condition (10) satisfies the following two requirements.

(1) The closed-loop system (12)–(14) should be asymptotically stable under the condition $\varepsilon(t) = 0$.

(2) $J(\varepsilon) < 0$ for all nonzero $\varepsilon(t)$ under the zero initial condition and a given $\gamma > 0$.

3. H_∞ Performance Analysis and Controller Design

3.1. Some Lemmas. Before giving the main theorems, we need the following two lemmas.

Lemma 1 (see [33]). *For any constant matrix $Q \in \mathbb{R}^{n \times n}$, $Q > 0$, scalars $\tau_1 \leq \tau(t) \leq \tau_3$, and vector function $\dot{x} : [-\tau_3, -\tau_1] \to \mathbb{R}^n$ such that the following integration is well defined, then it holds that*

$$\begin{aligned}&-\left(\tau_3 - \tau_1\right) \int_{t-\tau_3}^{t-\tau_1} \dot{x}^T\left(s\right) Q \dot{x}\left(s\right) ds \\ &\leq \zeta_1^T\left(t\right) \begin{bmatrix} -Q & * & * \\ Q & -2Q & * \\ 0 & Q & -Q \end{bmatrix} \zeta_1\left(t\right),\end{aligned} \tag{17}$$

where $\zeta_1^T(t) = \left[x^T(t-\tau_1) \;\; x^T(t-\tau(t)) \;\; x^T(t-\tau_3)\right]$.

Lemma 2 (see [34]). *For matrices $R > 0$ and $X^T = X$, one has*

$$-XR^{-1}X \leq \rho^2 R - 2\rho X, \tag{18}$$

where ρ is any chosen constant.

3.2. H_∞ Performance Analysis and Controller Design. Based on the Lyapunov functional method, we conclude the following results. Different from [17–19] in which free weighing matrix method is used, we use Jensen inequality approach to H_∞ performance analysis and H_∞ controller design. Reference [35] has theoretically proved that both of the methods are equivalent. However, using Jensen inequality can decrease decision variables and is easy for computation of LMI.

Theorem 3. *For given parameters σ, γ and matrix K, the system* (12)–(14) *under the event-triggered scheme* (15) *can keep on the internal stability and also the external disturbance rejection index γ, if there exist positive definite matrices P, Q, R, and Ω, such that the following matrix inequality holds:*

$$\begin{bmatrix} \Phi_{11} & * & * & * \\ \Phi_{21} & -\gamma^2 I & * & * \\ \Phi_{31} & \tau_M R B_2 & -R & * \\ \Phi_{41} & 0 & 0 & -I \end{bmatrix} < 0, \tag{19}$$

where

$$\begin{aligned} \Phi_{11} &= \begin{bmatrix} PA + A^T P + Q - R & * & * & * \\ K^T B^T P + R & \sigma\Omega - 2R & * & * \\ 0 & R & -R - Q & * \\ K^T B^T P & 0 & 0 & -\Omega \end{bmatrix} \\ \Phi_{21} &= \begin{bmatrix} B_2^T P & 0 & 0 & 0 \end{bmatrix} \\ \Phi_{31} &= \begin{bmatrix} \tau_M RA & \tau_M RBK & 0 & \tau_M RBK \end{bmatrix} \\ \Phi_{41} &= \begin{bmatrix} C & DK & 0 & DK \end{bmatrix}. \end{aligned} \tag{20}$$

Proof. Construct a Lyapunov functional as

$$\begin{aligned} V(t) = {} & x^T(t) P x(t) + \int_{t-\tau_M}^{t} x^T(s) Q x(s)\, ds \\ & + \tau_M \int_{t-\tau_M}^{t} \int_{s}^{t} \dot{x}^T(v) R \dot{x}(v)\, dv\, ds, \end{aligned} \tag{21}$$

where $P > 0$, $Q > 0$, and $R > 0$. For $t \in [t_m + \tau_m, t_{m+1} + \tau_{m+1})$, taking the time derivation on (21),

$$\begin{aligned} \dot{V}(t) = {} & 2x^T(t) P \left[Ax(t) + BKx(t - \tau(t)) \right. \\ & \left. + BKe_m(t) + B_2 \varepsilon(t) \right] + x^T(t) Q x(t) \\ & - x^T(t - \tau_M) Q x(t - \tau_M) + \tau_M^2 \dot{x}^T(t) R \dot{x}(t) \\ & - \tau_M \int_{t-\tau_M}^{t} \dot{x}^T(s) R \dot{x}(s)\, ds. \end{aligned} \tag{22}$$

Applying Lemma 1, we have

$$\begin{aligned} & -\tau_M \int_{t-\tau_M}^{t} \dot{x}^T(s) R \dot{x}(s)\, ds \\ & \le \zeta^T(t) \begin{bmatrix} -R & * & * \\ R & -2R & * \\ 0 & R & -R \end{bmatrix} \zeta(t), \end{aligned} \tag{23}$$

where $\zeta^T(t) = \left[x^T(t) \;\; x^T(t - \tau(t)) \;\; x^T(t - \tau_M) \right]$. Considering (22) and (15), we can obtain that

$$\begin{aligned} \dot{V}(t) \le {} & \xi^T(t) \Pi_1 \xi(t) + z^T(t) z(t) \\ & - \gamma^2 \varepsilon^T(t) \varepsilon(t) \\ & - z^T(t) z(t) + \gamma^2 \varepsilon^T(t) \varepsilon(t), \end{aligned} \tag{24}$$

where

$$\begin{aligned} \xi^T(t) &= \left[\zeta^T(t) \;\; e_m^T(t) \;\; \varepsilon^T(t) \right] \\ \Pi_1 &= \begin{bmatrix} \Phi_{11} + \Phi_{31}^T R^{-1} \Phi_{31} & * \\ \Phi_{21} + \tau_M B_2^T R \Phi_{31} & \tau_M^2 B_2^T R B_2 \end{bmatrix}. \end{aligned} \tag{25}$$

Combining (13) and (24), one can conclude that

$$\begin{aligned} \dot{V}(t) \le {} & \xi^T(t) \Pi_2 \xi(t) - z^T(t) z(t) \\ & + \gamma^2 \varepsilon^T(t) \varepsilon(t), \end{aligned} \tag{26}$$

where

$$\Pi_2 = \Pi_1 + \begin{bmatrix} \Phi_{41}^T \Phi_{41} & * \\ 0 & -\gamma^2 I \end{bmatrix}. \tag{27}$$

From (19) and by Schur complement, one can conclude from (26) that, for $t \in [t_m + \tau_m, t_{m+1} + \tau_{m+1})$,

$$\dot{V}(t) \le -z^T(t) z(t) + \gamma^2 \varepsilon^T(t) \varepsilon(t). \tag{28}$$

Since $\cup_{m=0}^{\infty} [t_m + \tau_m, t_{m+1} + \tau_{m+1}) = [0, \infty)$, $V(t)$ is continuous in t since $x(t)$ is continuous in t. Therefore, on both sides of (26), the integral from 0 to ∞ with respect to t yields

$$\begin{aligned} & V(\infty) - V(0) \\ & \le \int_0^{\infty} \left[-z^T(s) z(s) + \gamma^2 \varepsilon^T(s) \varepsilon(s) \right] ds. \end{aligned} \tag{29}$$

Under zero initial conditions, the following can be obtained:

$$\int_0^{\infty} \left[z^T(s) z(s) - \gamma^2 \varepsilon^T(s) \varepsilon(s) \right] ds \le 0. \tag{30}$$

That is $J(\varepsilon) < 0$. This completes the proof. □

In order to ensure the damping control performance under the circumstance of time delay of wide-area state feedback with event-triggered scheme and external disturbance, the main result is summarized in the following theorem, which can be derived based on Theorem 3.

Theorem 4. *For given parameters σ and γ, the system* (12)–(14) *under the event-triggered scheme* (15) *with $\Omega = X^{-1} \overline{\Omega} X^{-1}$ can keep on the internal stability and also the external disturbance rejection index γ, if there exist positive definite matrices X, $\overline{Q}$, $\overline{R}$, $\overline{\Omega}$, and Y of appropriate dimensions such that the following matrix inequality is feasible. Moreover, the*

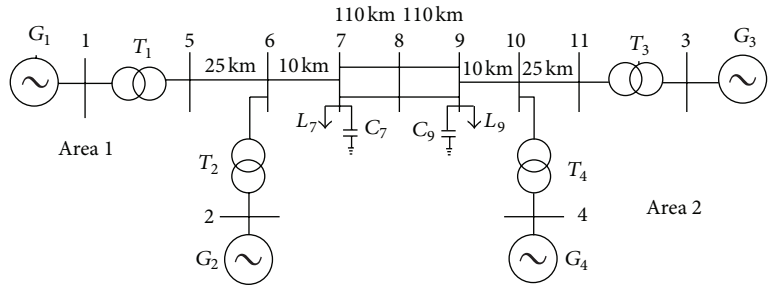

Figure 2: Two-area four-machine system.

gain matrix of such H_∞ damping controller can be obtained as $K = YX^{-1}$:

$$\begin{bmatrix} \overline{\Phi}_{11} & * & * & * \\ \overline{\Phi}_{21} & -\gamma^2 I & * & * \\ \overline{\Phi}_{31} & \tau_M B_2 & \overline{R} - 2X & * \\ \overline{\Phi}_{41} & 0 & 0 & -I \end{bmatrix} < 0, \tag{31}$$

where

$$\Phi_{11} = \begin{bmatrix} AX + XA^T + \overline{Q} - \overline{R} & * & * & * \\ Y^T B^T + \overline{R} & \sigma\overline{\Omega} - 2\overline{R} & * & * \\ 0 & \overline{R} & -\overline{R} - \overline{Q} & * \\ Y^T B^T & 0 & 0 & -\overline{\Omega} \end{bmatrix} \tag{32}$$

$$\Phi_{21} = \begin{bmatrix} B_2^T & 0 & 0 & 0 \end{bmatrix} \tag{33}$$

$$\Phi_{31} = \begin{bmatrix} \tau_M AX & \tau_M BY & 0 & \tau_M BY \end{bmatrix} \tag{34}$$

$$\Phi_{41} = \begin{bmatrix} CX & DY & 0 & DY \end{bmatrix}. \tag{35}$$

Proof. Defining $X = P^{-1}$, pre- and postmultiplying (19) with $\mathrm{diag}\{X, X, X, X, I, R^{-1}, I\}$, making the following changes in the variables: $\overline{R} = XRX$, $\overline{Q} = XQX$, $\overline{\Omega} = X\Omega X$, $Y = KX$, and using Lemma 2 and Schur complement, (31) is derived from (19). □

4. Results of Case Studies

This section aims to validate the proposed wide-area H_∞ damping controller design method with event-triggered scheme. There are different performance indices to evaluate the wide-area H_∞ damping controller, and there are two parameters, that is, event-triggering parameter σ and disturbance rejection index γ that should be chosen appropriately. In this section, we focus on the time response of the power system with small signal, release times of sampled state signals during a certain simulation time, maximum allowable delay time (delay margin), and disturbance rejection level. To find the appropriate σ and γ, a series of numeric experiments is carried out through the application of WAHDC to the four-machine two-area test system, which is also the benchmark system for the oscillation damping study [30]. Figure 2 shows the four-machine two-area system. The detailed parameters can be found in [30].

In the following simulations, the state-space description of the power system is based on model (8), that is, the relative power angle synchronized reference frame model. The matrices A and B can be established by the modeling method mentioned previously at the given operating point. For regulated output, we set the weighting matrices $C = \mathrm{diag}\{10, 1.0, 10, 1, 10, 1, 10, 0.5, 0.5, 0.5\}$ and D as

$$D = \begin{bmatrix} 0 & 0 & 0 & 0 \\ 0 & 0 & 0 & 0 \\ 0 & 0 & 0 & 0 \\ 0 & 0 & 0 & 0 \\ 0 & 0 & 0 & 0 \\ 0 & 0 & 0 & 0 \\ 0 & 0 & 0 & 0 \\ 1 & 0 & 0 & 0 \\ 0 & 1 & 0 & 0 \\ 0 & 0 & 1 & 0 \\ 0 & 0 & 0 & 1 \end{bmatrix}. \tag{36}$$

And also we choose $B_2 = D$. For the convenience of analysis, the state variables are reordered as

$$x = \begin{bmatrix} \Delta\omega_1 & \Delta\delta_{14} & \Delta\omega_2 & \Delta\delta_{24} & \Delta\omega_3 & \Delta\delta_{34} & \Delta\omega_4 & \Delta E'_{q1} & \Delta E'_{q2} & \Delta E'_{q3} & \Delta E'_{q4} \end{bmatrix}^T. \tag{37}$$

The duration of all the following simulations is always 30 s.

4.1. Case Study about the Influence of σ on System Time Response and Network Utilization. A time domain analysis method of the closed-loop system is carried out to reveal the performance of the proposed controller in terms of improving the damping of interarea oscillation. The exogenous disturbance is assumed to be

$$\varepsilon_1(t) = \begin{cases} 0.1\,\mathrm{sign}(\sin t), & \text{if} \quad t \in [0, 5] \\ 0, & \text{otherwise} \end{cases} \tag{38}$$
$$\varepsilon_i(t) = 0, \quad i = 2, 3, 4.$$

Table 1: Network utilization for different σ.

Event trigger parameter σ	0	0.1	0.2	0.3
The maximum interevent interval (s)	0.02	0.8800	1.400	2.4800
The average interevent interval (s)	0.02	0.0932	0.1235	0.1587
Total release times	1501	322	243	189
Release rate α	100%	21.45%	16.19%	12.59%

Table 2: IAEs for different σ.

Event trigger parameter σ	0.1	0.2	0.3
IAEs ($\Delta\delta_{14}$ deg)	7.9109	11.0344	21.5632
IAEs ($\Delta\omega_3$ p.u.)	0.0039	0.0066	0.0113

The damping action of the H_∞ controller is examined under different event-triggering parameter σ. According to the time-delay analysis of WAMS in [36, 37], we set $\tau_M = 0.08$ s, $h = 0.02$ s, and then the transmission delay $\overline{\tau}$ is 0.06 s correspondingly. For $\gamma = 20$, the dynamic response with different σ chosen from the feasible range, which is shown in Figure 7 and will be described in detail later, is displayed in Figures 3 and 4, and the corresponding network utilization is reported in Table 1. The data transmission rate $\alpha = N/N_0 \times 100\%$ is also listed in Table 1, where N_0 denotes the number of total measured data release times with $\sigma = 0$, and N indicates the number of release times with $\sigma \neq 0$.

To illustrate the quality of the systems response, we introduce two indices, that is, the integrated absolute error (IAE) between the system response of periodic release (or time-based) strategy and event-triggered scheme [38] and the time response of the error (TRE) between the time-based strategy and the event-triggered scheme, where

$$\text{IAE} = \int_0^t \left| x_{\text{time-based}}(t) - x_{\text{event-triggered}}(t) \right| dt, \quad (39)$$

$$\text{TRE} = x_{\text{time-based}}(t) - x_{\text{event-triggered}}(t). \quad (40)$$

The TREs and IAEs for different σ are illustrated in Figures 5 and 6 and Table 2, respectively. In Figure 5, $\Delta\delta_{14_0}$ denotes the relative angle between G_1 and G_4 with time-based strategy, and $\Delta\delta_{14_i}$ represents the relative angle between G_1 and G_4 with different σ_i, $i = 1, 2, 3$, where $\sigma_1 = 0.1$, $\sigma_2 = 0.2$, and $\sigma_3 = 0.3$. In Figure 6, $\Delta\omega_{3_i}$, $i = 0, 1, 2, 3$ has similar meaning.

The curves depicted in Figures 3 and 4 show that the oscillation between Area 1 and Area 2 is damped quickly for different event-triggering parameter σ. Even when $\sigma = 0.3$, the oscillation is damped well. It shows that the WAHDC with event-triggered scheme can provide effective damping of interarea oscillations when the power system is subjected to external interference and communication time delay exists in the damping control loop. Moreover, from Table 1, it is found that the times when the sampled signals are released to be used to calculate the control output at the control center decrease with the increase of σ. It can be seen from the last row of Table 1 that, for $\sigma = 0.1, 0.2, 0.3$, with event-triggered scheme, only 21.45%, 16.19%, and 12.59% of measured states need to be released to the WAHDC, respectively. In other words, the network utilization by the event-triggered scheme

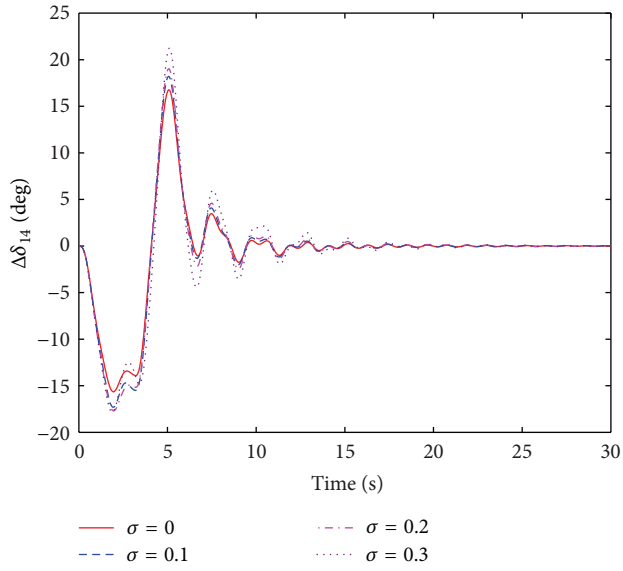

Figure 3: Dynamic response of relative angle between G_1 and G_4 for different σ.

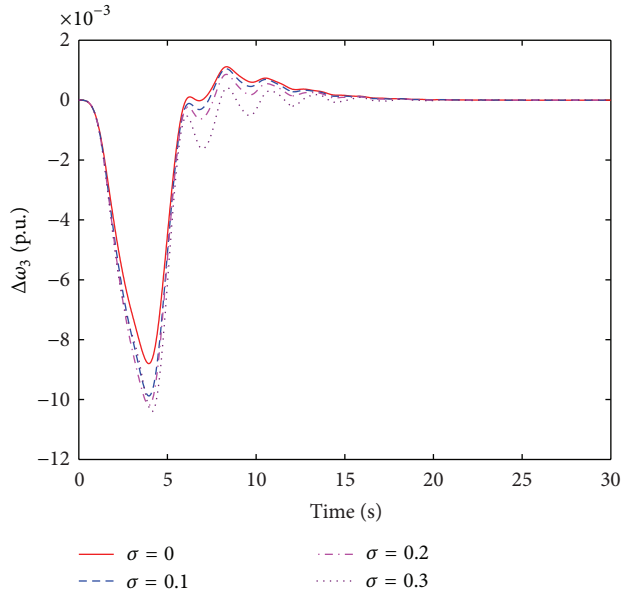

Figure 4: Dynamic response of angular velocity deviation of G_3 for different σ.

can be obtained by 78.55%, 83.81%, and 87.41% improvement, respectively. Thus the burden of the network communication between control center and the actuators widely distributed is reduced and the communication bandwidth is saved. That validates the effectiveness of the design approach.

However, according to the definition of IAE we can see a lower value of IAE meaning that the control strategy provides a better damping performance. The data in Table 2 show that the dynamic response is degraded to a certain degree with increase of σ; that is, it is expected that larger σ will yield larger IAE with less network utilization. From the point of view of WAHDC design, the relationship between event

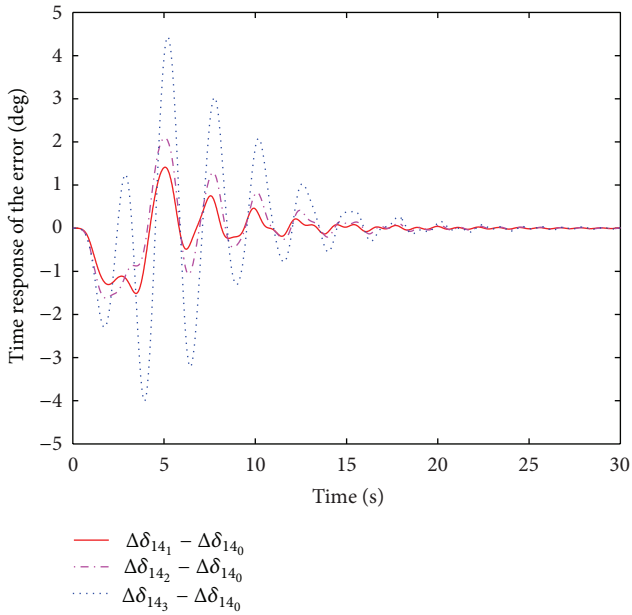

Figure 5: Time response of the error between time-based strategy and event-triggered scheme ($\Delta\delta_{14}$).

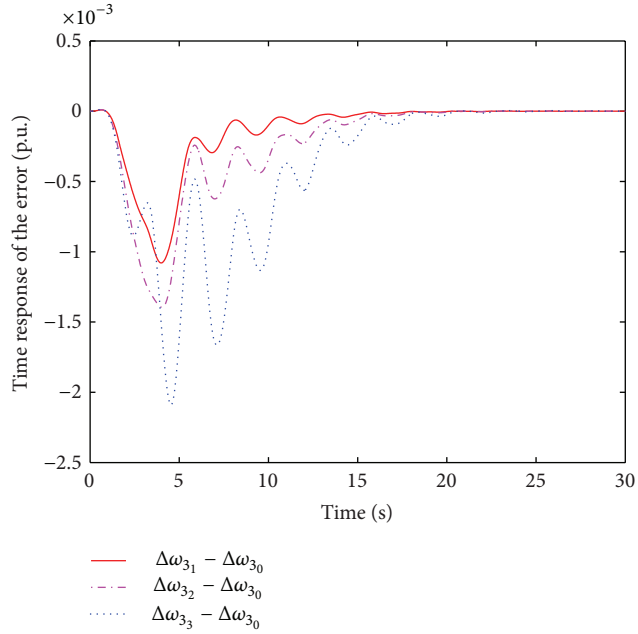

Figure 6: Dynamic response of the error between time-based strategy and event-triggered scheme ($\Delta\omega_3$).

Table 3: Delay margin for different σ.

σ	0	0.1	0.2	0.3	0.4	0.5	0.6	0.7
$\gamma = 20$	0.131	0.109	0.094	0.085	0.015	—	—	—
$\gamma = 30$	0.140	0.121	0.111	0.101	0.093	0.083	0.018	—
$\gamma = 40$	0.143	0.123	0.116	0.108	0.100	0.091	0.078	0.020

Table 4: Smallest γ for different σ.

σ	0	0.1	0.2	0.3	0.4	0.5	0.6	0.69	0.8
$\tau_M = 0.06$ s	11	14	16	19	22	26	33	43	148
$\tau_M = 0.08$ s	11	14	16	19	24	30	43	118	—

trigger parameter σ and network utilization can provide an effective guide for the design of WAHDC, and the event-triggering parameter can be chosen to achieve trade-off between the network utilization and damping performance for certain delay margin and perturbation attenuation index.

As stated previously, for certain delay margin and perturbation attenuation index, event trigger parameter σ can be chosen in a feasible range. The following studies are aimed at finding the feasible range.

4.2. Case Study about the Relationship between σ and Time Delay. In this section, simulation studies are carried out to find a guiding method to choose an appropriate σ for certain γ. For given time delay and γ, a feasible range of σ can be found by manually increasing the value of σ and checking the feasibility of (31). The upper bound of σ is calculated by selecting different sets of τ_M and γ. In other words, the delay margin that resulted from different σ and γ can also be obtained in similar way. Results of the upper bound of σ with respect to different τ_M and the delay margin for different σ are shown in Figure 7 and Table 3 separately.

Results in Figure 7 show that, for a certain γ, the curve declines slowly at first and after a turning point it declines sharply with the increase of τ_M. The trend of the relationship between τ_M and the upper bound of σ for different γ is similar except that with the increase of γ, the value of the upper bound of σ decreases for the same τ_M. Namely, with the increase of τ_M, one can choose a σ in an increasing feasible range. From another perspective, from Table 3 we can also conclude that for given γ, increasing the value of σ, delay margin of WAHDC decreases. Thus for the full use of network bandwidth one can choose a larger σ. For example, for $\gamma = 30$, one can choose σ from 0 to about 0.6 when the maximum delay in damping control loop is 0.08 s. However, as addressed previously, considering the damping performance and delay margin of the controller, the value of σ cannot be too large.

4.3. Case Study about the Relationship between σ and the Disturbance Rejection Level γ. Different selection of disturbance rejection level γ also influences the feasible range of σ. The relationship between σ and the disturbance rejection level γ is investigated in this section. By applying Theorem 4, we can get the upper bound of σ for different set of γ and time delays and also obtain the smallest γ for certain combination of σ and time delay. Results of upper bound of σ with respect to different γ and the smallest γ for different σ and time delay are shown in Figure 8 and Table 4 separately.

As is well known, for H_∞ control problem, smaller γ means better disturbance rejection level. However, from Figure 8 and Table 4 we can know that, when γ is set to less than 40, the feasible range of σ decreases rapidly for both 0.06 s and 0.08 s time delay. Since larger σ means less network

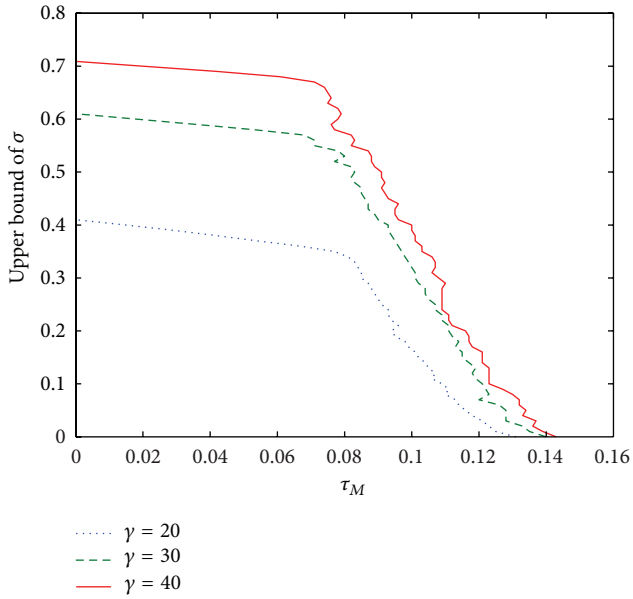

Figure 7: Upper bound of σ for different τ_M.

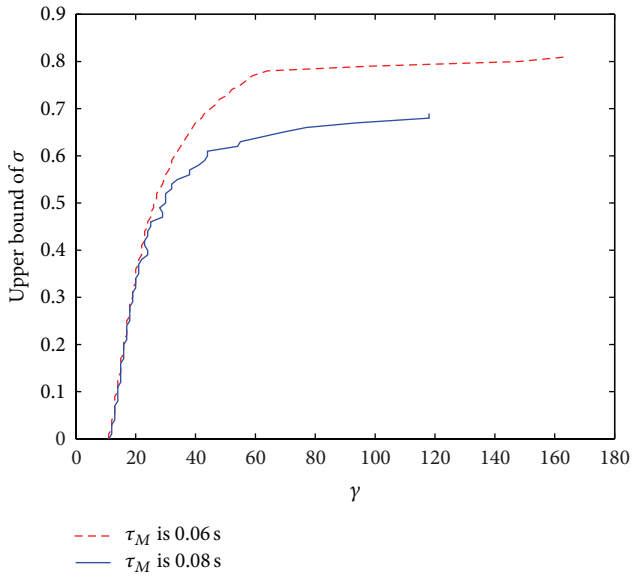

Figure 8: Upper bound of σ for different γ.

overheads generally, for reduction of network overheads, the value of γ cannot be set too small. Moreover, when $\sigma = 0$ we can know the smallest value of γ for given time delay. Therefore, the findings can provide an effective guide for the WAHDC design for certain disturbance rejection performance and delay margin to achieve full use of network resource.

5. Conclusion and Future Work

A centralized H_∞ wide-area damping controller for multimachine power system is proposed in this paper. Besides using the wide-area signals from remote generators to improve the damping of the interarea oscillation in the power system, to reduce the amount of data transfer, an event-triggered scheme is introduced. Moreover, an H_∞ control criterion is obtained for the controller design based on the Jensen inequality and LMI approach. By solving a set of LMIs, Theorem 4 provides a useful way of design for feedback gain with given trigger parameter σ. Then to validate the presented WAHDC with event-triggered scheme and to find the method to choose an appropriate event trigger parameter σ, case studies are carried out based on the two-area four-machine power system. From the simulation results, the following conclusion can be drawn.

(i) The presented WAHDC with event-triggered scheme can damp the interarea oscillation effectively when the disturbance is energy bounded. Increasing the value of σ in the feasible range can deduce the traffic volume between WAHDC and machines. But the dynamic response of power system under WAHDC is degenerated to some extent.

(ii) The introduction of event-triggered scheme has some influence on system dynamic performance, network utilization, delay margin, and disturbance rejection level. In view of WAHDC design, increasing the value of σ can decrease the delay margin and disturbance rejection performance. Findings from previous simulations give a guiding method to select appropriate σ to get compromise between damping performance, network utilization, delay margin, and disturbance rejection level.

The previous researches are promising, but also have some limits. The real power system is nonlinear and of high dimensionality, and it is neither practical nor necessary to design the full state feedback controller based on the linearized model. Further research is still needed to combine the model reduction theory and the event-triggered scheme presented in this paper. Furthermore, the proposed WAHDC with event-triggered scheme only reduces the data transfer from control center to distributed machines. Another direction of our future research is to construct distributed event detectors at the PMUs side to reduce the whole network overheads. In addition, the algorithm and method proposed in [39, 40] may be used to find the optimal value of σ.

Symbols

$\delta_i(t)$: Power angle of the ith generator, in deg
$\omega_i(t)$: The angular velocity of the ith generator, in p.u.
ω_0: Synchronous machine speed, in p.u.
$E'_{qi}(t)$: q-axis transient potential, in p.u.
$E_f(t)$: Control input, excitation voltage, in p.u.
x_{di}: d-axis synchronous reactance, in p.u.
x'_{di}: d-axis transient reactance, in p.u.

$Y_{ij} = G_{ij} + jB_{ij}$: Modulus of the transfer admittance between the ith and jth generator, in p.u.
P_m: Mechanical input power, in p.u., which is a constant
P_e: Electrical power, in p.u.
D_i: Damping coefficient of ith generator
M_i: Stored energy at rated speed, inertia constant, in seconds
T'_{d0}: d-axis open circuit transient timeconstant, in seconds
I_{di}: Direct axis current, in p.u.
I_{qi}: Quadrature axis current, in p.u.

Acknowledgments

The authors would like to thank the anonymous reviewers for providing their valuable comments and constructive suggestions that have improved the presentation of this paper. This work was supported by the National Natural Science Foundation of China (nos. 60834002 and 61074025) and the Ph. D. Programs Foundation of Ministry of Education of China (no. 20110142110036).

References

[1] J. Ma, T. Wang, J. Thorp, A. Phadke, and Z. Wang, "Application of wide-area collocated control technique for damping inter-area oscillations using flexible ac transmission systems devices," *Electric Power Components and Systems*, vol. 39, no. 13, pp. 1452–1467, 2011.

[2] Y. Zhang and A. Bose, "Design of wide-area damping controllers for interarea oscillations," *IEEE Transactions on Power Systems*, vol. 23, no. 3, pp. 1136–1143, 2008.

[3] X. Yang and A. Feliachi, "Stabilization of inter-area oscillation modes through excitation," *IEEE Transactions on Power Systems*, vol. 9, no. 1, pp. 494–502, 1994.

[4] J. H. Chow, J. J. Sanchez-Gasca, H. Ren, and S. Wang, "Power system damping controller design," *IEEE Control Systems Magazine*, vol. 20, no. 4, pp. 82–90, 2000.

[5] R. Grondin, I. Kamwa, G. Trudel, L. Gérin-Lajoie, and J. Taborda, "Modeling and closed-loop validation of a new PSS concept, the Multi-Band PSS," in *Proceedings of IEEE Power Engineering Society General Meeting*, pp. 1804–1809, IEEE, July 2003.

[6] H. Ni, G. T. Heydt, and L. Mili, "Power system stability agents using robust wide area control," *IEEE Transactions on Power Systems*, vol. 17, no. 4, pp. 1123–1131, 2002.

[7] X. Xie and C. Lu, "Optimization and coordination of wide-area damping controls for enhancing the transfer capability of interconnected power systems," *Electric Power Systems Research*, vol. 78, no. 6, pp. 1099–1108, 2008.

[8] H. Golestani Far, H. Banakar, P. Li, C. Luo, and B. T. Ooi, "Damping interarea oscillations by multiple modal selectivity method," *IEEE Transactions on Power Systems*, vol. 24, no. 2, pp. 766–775, 2009.

[9] D. Dotta, A. S. e Silva, and I. C. Decker, "Wide-area measurements-based two-level control design considering signal transmission delay," *IEEE Transactions on Power Systems*, vol. 24, no. 1, pp. 208–216, 2009.

[10] B. Chaudhuri, R. Majumder, and B. C. Pal, "Wide-area measurement-based stabilizing control of power system considering signal transmission delay," *IEEE Transactions on Power Systems*, vol. 19, no. 4, pp. 1971–1979, 2004.

[11] S. A. Nezam, A. S. Dobakhshari, S. Azizi, and A. M. Ranjbar, "A sectionalizing method in power system restoration based on WAMS," *IEEE Transactions on Smart Grid*, vol. 2, no. 1, pp. 178–185, 2011.

[12] R. Eriksson and L. Söder, "Wams based identification for obtaining linear models to coordinate controllable devices," *Electrical Engineering*, pp. 1–10, 2012.

[13] J. Zhang, J. Y. Wen, S. J. Cheng, and Z. Y. Dong, "Realization of the WAMS based power system aggregate load area model," in *Proceedings of IEEE Power and Energy Society General Meeting: Conversion and Delivery of Electrical Energy in the 21st Century (PES '08)*, IEEE, July 2008.

[14] Z. Wang, Y. Zhang, and J. Zhang, "Principal components fault location based on wams/pmu measure system," in *Proceedings of Power and Energy Society General Meeting*, pp. 1–5, IEEE, 2011.

[15] D. Li, R. Li, Y. Sun, and H. Chen, "State estimation with WAMS/SCADA hybrid measurements," in *Proceedings of IEEE Power and Energy Society General Meeting (PES '09)*, pp. 1–5, IEEE, July 2009.

[16] S. Hu and D. Yue, "Event-triggered control design of linear networked systems with quantizations," *ISA Transactions*, vol. 51, no. 1, pp. 153–162, 2012.

[17] S. Hu, Y. Zhang, and Z. Du, "Network-based H_∞ tracking control with event-triggering sampling scheme," *IET Control Theory & Applications*, vol. 6, no. 4, pp. 533–544, 2012.

[18] D. Yue, E. Tian, and Q. L. Han, "A delay system method to design of event-triggered control of networked control systems," in *Proceedings of the 50th IEEE Conference on Decision and Control and European Control Conference (CDC-ECC '11)*, pp. 1668–11673, December 2011.

[19] D. Yue, E. Tian, and Q. Han, "A delay system method for designing event-triggered controllers of networked control systems," *IEEE Transactions on Automatic Control*, vol. 58, no. 2, pp. 475–481, 2013.

[20] K. J. Astrom and B. M. Bernhardsson, "Comparison of Riemann and Lebesgue sampling for first order stochastic systems," in *Proceedings of the 41st IEEE Conference on Decision and Control*, vol. 2, pp. 2011–2016, IEEE, December 2002.

[21] E. Kofman and J. H. Braslavsky, "Level crossing sampling in feedback stabilization under data-rate constraints," in *Proceedings of the 45th IEEE Conference on Decision and Control (CDC '06)*, pp. 4423–4428, IEEE, December 2006.

[22] P. G. Otanez, J. R. Moyne, and D. M. Tilbury, "Using deadbands to reduce communication in networked control systems," in *Proceedings of American Control Conference*, vol. 4, pp. 3015–3020, IEEE, 2002.

[23] M. Miskowicz, "Send-on-delta concept: an event-based data reporting strategy," *Sensors*, vol. 6, no. 1, pp. 49–63, 2006.

[24] X. Wang and M. D. Lemmon, "Self-triggered feedback control systems with finite-gain $\mathscr{L}_2$ stability," *IEEE Transactions on Automatic Control*, vol. 54, no. 3, pp. 452–467, 2009.

[25] V. Nguyen and Y. Suh, "Networked estimation with an area-triggered transmission method," *Sensors*, vol. 8, no. 2, pp. 897–909, 2008.

[26] X. Xiao, F. Wang, and H. Zhao, "Application of self-triggered control in power system excitation control," in *Proceedings of International Conference on Electrical and Control Engineering (ICECE '11)*, pp. 577–580, IEEE, 2011.

[27] N. Kashyap, S. Werner, and Y. Huang, "Event-triggered multi-area state estimation in power systems," in *Proceedings of the 4th IEEE International Workshop on Computational Advances in Multi-Sensor Adaptive Processing (CAMSAP '11)*, pp. 133–136, IEEE, 2011.

[28] S. Li, D. Sauter, and B. Xu, "Fault isolation filter for networked control system with event-triggered sampling scheme," *Sensors*, vol. 11, no. 1, pp. 557–572, 2011.

[29] E. Tian, D. Yue, and Z. Gu, "Robust H_∞ control for nonlinear systems over network: a piecewise analysis method," *Fuzzy Sets and Systems*, vol. 161, no. 21, pp. 2731–2745, 2010.

[30] P. Kundur, N. Balu, and M. Lauby, *Power System Stability and Control*, vol. 4, McGraw-Hill, New York, NY, USA, 1994.

[31] D. Gan, Z. Qu, and H. Cai, "Multi machine power system excitation control design via theories of feedback linearization control and nonlinear robust control," *International Journal of Systems Science*, vol. 31, no. 4, pp. 519–527, 2000.

[32] Y. Ni, B. Zhang, and S. Chen, *Dynamic Power System Theory and Analysis*, Tsinghua University Press, Beijing, China, 2002.

[33] C. Peng, D. Yue, E. Tian, and Z. Gu, "A delay distribution based stability analysis and synthesis approach for networked control systems," *Journal of the Franklin Institute*, vol. 346, no. 4, pp. 349–365, 2009.

[34] H. K. Lam and L. D. Seneviratne, "Tracking control of sampled-data fuzzy-model-based control systems," *IET Control Theory and Applications*, vol. 3, no. 1, pp. 56–67, 2009.

[35] S. Xu and J. Lam, "On equivalence and efficiency of certain stability criteria for time-delay systems," *IEEE Transactions on Automatic Control*, vol. 52, no. 1, pp. 95–101, 2007.

[36] J. W. Stahlhut, T. J. Browne, G. T. Heydt, and V. Vittal, "Latency viewed as a stochastic process and its impact on wide area power system control signals," *IEEE Transactions on Power Systems*, vol. 23, no. 1, pp. 84–91, 2008.

[37] P. Li, X. Wu, C. Lu et al., "Implementation of CSG's wide-area damping control system: overview and experience," in *Proceedings of IEEE/PES Power Systems Conference and Exposition (PSCE '09)*, pp. 1–9, March 2009.

[38] J. Sánchez, M. Guarnes, and S. Dormido, "On the application of different event-based sampling strategies to the control of a simple industrial process," *Sensors*, vol. 9, no. 9, pp. 6795–6818, 2009.

[39] Y. Tang, H. Gao, J. Kurths, and J. Fang, "Evolutionary pinning control and its application in uav coordination," *IEEE Transactions on Industrial Informatics*, vol. 8, no. 4, pp. 828–838, 2012.

[40] Y. Tang and W. K. Wong, "Distributed synchronization of coupled neural networks via randomly occurring control," *IEEE Transactions on Neural Networks and Learning Systems*, vol. 24, no. 3, pp. 435–447, 2013.